Dynamical Systems Tools Applied to Transfer Orbits in Spacecraft Mission Design

Josep J. Masdemont, E. Canalias

Dept. Matemàtica Aplicada I. Universitat Politècnica de Catalunya

Stability and Instability in Mechanical Systems:
Applications and Numerical Tools

Barcelona, December 1–5, 2008

Reference Problem. RTBP

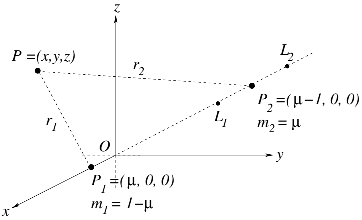

Differential equations:

$$
\begin{aligned}
\dot{x} &= p_x + y, & \dot{p}_x &= -\partial H/\partial x, \\
\dot{y} &= p_y - x, & \dot{p}_y &= -\partial H/\partial y, \\
\dot{z} &= p_z, & \dot{p}_z &= -\partial H/\partial z.
\end{aligned}
$$

Hamiltonian:

$$H(x, y, z, p_z, p_y, p_z) = \frac{1}{2}(p_x^2 + p_y^2 + p_z^2) - xp_y + yp_x - \frac{1-\mu}{r_1} - \frac{\mu}{r_2},$$

with

$$r_1 = \sqrt{(x-\mu)^2 + y^2 + z^2},\ r_2 = \sqrt{(x-\mu+1)^2 + y^2 + z^2}.$$

Jacobi first integral:

$$C = -2H + \mu(1-\mu).$$

The RTBP in synodical coordinates

$$\begin{aligned} X'' - 2Y' &= \Omega_X, \\ Y'' + 2X' &= \Omega_Y, \\ Z'' &= \Omega_Z, \end{aligned}$$

where,

$$\Omega = \frac{1}{2}(X^2 + Y^2) + \frac{1-\mu}{R_1} + \frac{\mu}{R_2} + \frac{1}{2}\mu(1-\mu).$$

$$R_2^2 = (X + 1 - \mu)^2 + Y^2 + Z^2, \quad R_1^2 = (X - \mu)^2 + Y^2 + Z^2.$$

Jacobi constant:

$$C = 2\Omega(X, Y, Z) - (X'^2 + Y'^2 + Z'^2).$$

Libration Points in the RTBP

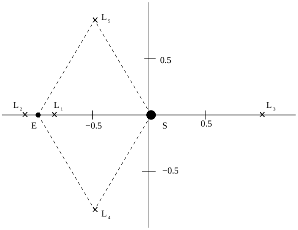

X coordinates of $L_{1,2}$ are,

$$X_i = -1 \pm \left(\frac{\mu}{3}\right)^{1/3} - \frac{1}{3}\left(\frac{\mu}{3}\right)^{2/3} + O(\mu), \quad i = 1, 2.$$

In the Earth–Sun system,

$$d(L_{1,2}, \text{Earth}) \approx 1.5 \cdot 10^6 \text{ km}, \qquad d(\text{Sun}, \text{Earth}) \approx 150 \cdot 10^6 \text{ km}.$$

Properties of Libration Point Orbits

- They are easy and inexpensive to reach from Earth.
- They provide good observation sites of the Sun.
- For missions with heat sensitive instruments, orbits around the L_2 point of the Sun–Earth system provide a constant geometry for observation with half of the entire celestial sphere available at all times, since the Sun, Earth and Moon are always behind the spacecraft.
- The communications system design is simple and cheap, since the libration orbits around the L_1 and L_2 points of the Sun–Earth system always remain close to the Earth, at a distance of roughly 1.5 million km with a near-constant communications geometry.

Properties of Libration Point Orbits

- The L_2 environment of the Sun–Earth system is highly favourable for non-cryogenic missions requiring great thermal stability, suitable for highly precise visible light telescopes.
- The libration orbits around the L_2 point of the Earth–Moon system, can be used to establish a permanent communications link between the Earth and the hidden part of the Moon.
- The libration point orbits can provide ballistic planetary captures, such as for the one used by the Hiten mission.

Properties of Libration Point Orbits

- The libration point orbits provide Earth transfer and return trajectories, such as the one used for the Genesis mission.
- The libration point orbits provide interplanetary transport which can be exploited in the Jovian and Saturn systems to design a low energy cost mission to tour several of their moons (Petit Grand Tour mission).
- Recent work has shown that formation flight with a rigid shape is possible about libration point orbits.

Poincaré map representation

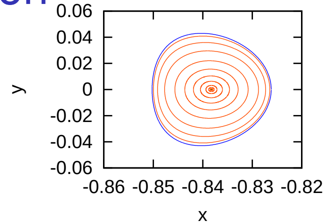

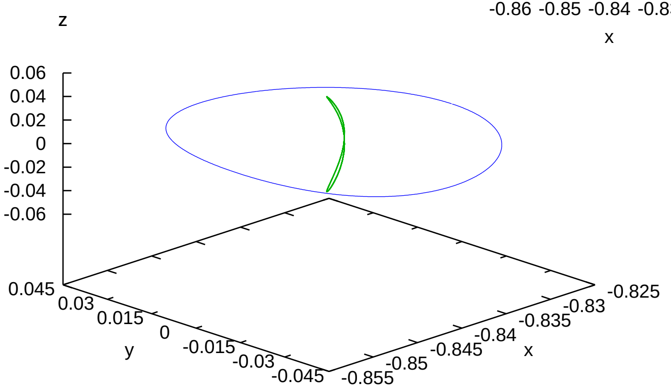

Poincaré map representation

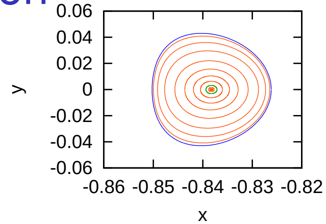

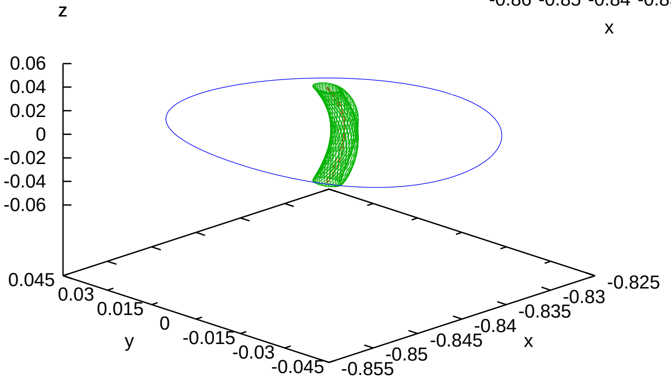

Poincaré map representation

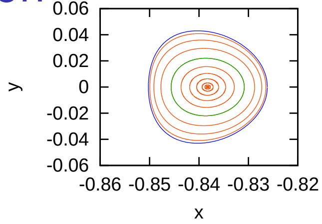

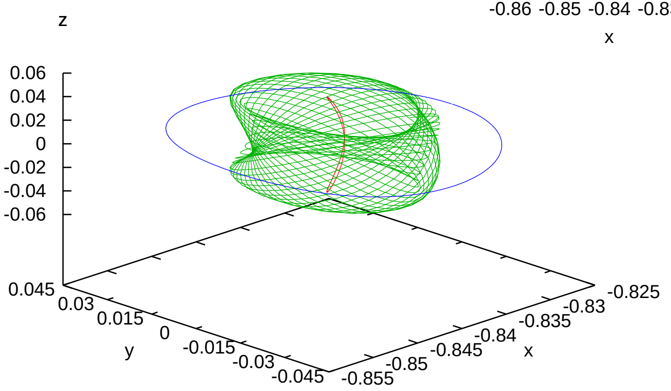

Poincaré map representation

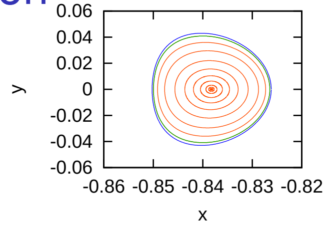

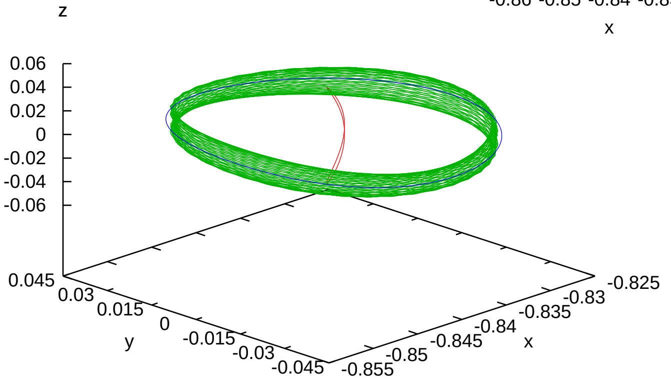

Poincaré map representation of LPO

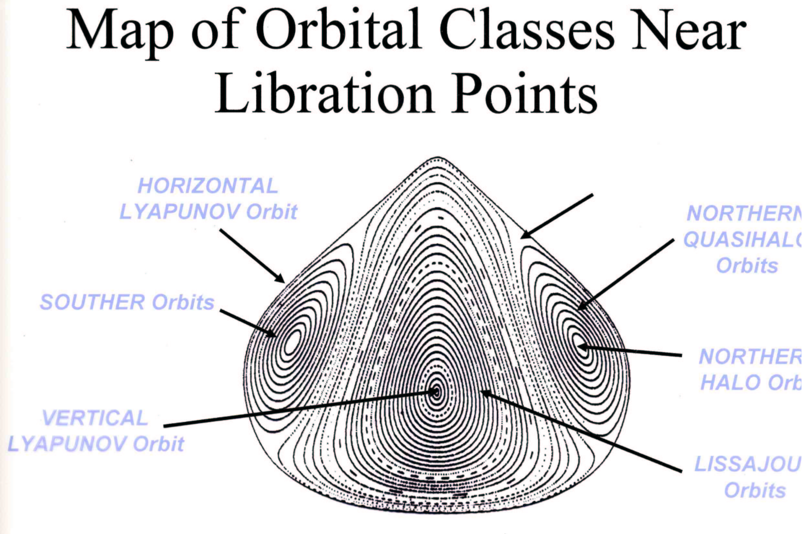

A Lindstedt-Poincaré Procedure

Computation of the Lissajous trajectories (2D tori) and halo orbits (1D tori or periodic orbits) with their invariant manifolds. The RTBP equations of motion can be written as

$$
\begin{aligned}
\ddot{x} - 2\dot{y} - (1 + 2c_2)x &= \frac{\partial}{\partial x} \sum_{n \geq 3} c_n \rho^n P_n\left(\frac{x}{\rho}\right), \\
\ddot{y} + 2\dot{x} + (c_2 - 1)y &= \frac{\partial}{\partial y} \sum_{n \geq 3} c_n \rho^n P_n\left(\frac{x}{\rho}\right), \\
\ddot{z} + c_2 z &= \frac{\partial}{\partial z} \sum_{n \geq 3} c_n \rho^n P_n\left(\frac{x}{\rho}\right),
\end{aligned}
$$

Eigenvalues at $L_{1,2}$ (RTBP/Hill)

The eigenvalues of the linear part of the flow at $L_{1,2}$ are

$\pm\lambda$	$\pm i\,\omega$	$\pm i\,\nu$
$\pm\sqrt{\frac{c_2-2+\sqrt{9c_2^2-8c_2}}{2}}$	$\pm\sqrt{\frac{2-c_2+\sqrt{9c_2^2-8c_2}}{2}}$	$\pm\sqrt{-c_2}$

so, the second order terms of the Hamiltonian in normal (diagonal) form are

$$H_2 = \lambda x p_x + \frac{\omega}{2}\left(y^2 + p_y^2\right) + \frac{\nu}{2}\left(z^2 + p_z^2\right),$$

and the equilibrium points $L_{1,2}$ behave as a

saddle $\times$ **centre** $\times$ **centre**

A Linsdtedt Poincaré Procedure

$$\left.\begin{array}{l} x(t) = \alpha_1 e^{\lambda_0 t} + \alpha_2 e^{-\lambda_0 t} + \alpha_3 \cos(\omega_0 t + \phi_1), \\ y(t) = \bar{k}_2 \alpha_1 e^{\lambda_0 t} - \bar{k}_2 \alpha_2 e^{-\lambda_0 t} + \bar{k}_1 \alpha_3 \sin(\omega_0 t + \phi_1), \\ z(t) = \alpha_4 \cos(\nu_0 t + \phi_2). \end{array}\right\}$$

- $\alpha_1 = \alpha_2 = 0$ gives linear Lissajous.
- $\alpha_1 = 0, \alpha_2 \neq 0$ defines **Stable Manifold**.
- $\alpha_2 = 0, \alpha_1 \neq 0$ defines **Unstable Manifold**.

The goal of our LP is to construct high order expansions with similar properties.

A Linsdtedt Poincaré Procedure

$$x(t) = \sum e^{(i-j)\theta_3} \Big[x^{pq}_{ijkm} \cos(p\,\theta_1 + q\,\theta_2) + \bar{x}^{pq}_{ijkm} \sin(p\,\theta_1 + q\,\theta_2) \Big] \alpha_1^i \alpha_2^j \alpha_3^k \alpha_4^m$$

$$y(t) = \sum e^{(i-j)\theta_3} \Big[y^{pq}_{ijkm} \cos(p\,\theta_1 + q\,\theta_2) + \bar{y}^{pq}_{ijkm} \sin(p\,\theta_1 + q\,\theta_2) \Big] \alpha_1^i \alpha_2^j \alpha_3^k \alpha_4^m$$

$$z(t) = \sum e^{(i-j)\theta_3} \Big[z^{pq}_{ijkm} \cos(p\,\theta_1 + q\,\theta_2) + \bar{z}^{pq}_{ijkm} \sin(p\,\theta_1 + q\,\theta_2) \Big] \alpha_1^i \alpha_2^j \alpha_3^k \alpha_4^m$$

where $\theta_1 = \omega t + \phi_1, \quad \theta_2 = \nu t + \phi_2, \quad \theta_3 = \lambda t$

and,

$$\omega = \sum \omega_{ijkm}\, \alpha_1^i \alpha_2^j \alpha_3^k \alpha_4^m, \quad \nu = \sum \nu_{ijkm}\, \alpha_1^i \alpha_2^j \alpha_3^k \alpha_4^m,$$
$$\lambda = \sum \lambda_{ijkm}\, \alpha_1^i \alpha_2^j \alpha_3^k \alpha_4^m.$$

A Linsdtedt Poincaré Procedure

Facts to save computer storage and CPU time.
Considering a series truncated at order (N_1, N_2).

- We consider always terms with $i, j, k, m > 0$ and $p > 0$.
- Always $i + j \leq N_1$, $k + m \leq N_2$ (and $i + j + k + m \leq N_2$ for a type I series).
- Always $p \leq k$ and $p \equiv k \pmod 2$.
- Always $|q| \leq m$ and $q \equiv m \pmod 2$ and in case that $p = 0$, only terms with $q \geq 0$ must be kept.
- Coefficients x_{ijkm}^{pq}, $\bar{x}_{ijkm}^{pq}$, y_{ijkm}^{pq} and $\bar{y}_{ijkm}^{pq}$ are zero when m is odd.
- Coefficients z_{ijkm}^{pq} and $\bar{z}_{ijkm}^{pq}$ are zero when m is even.

A Linsdtedt Poincaré Procedure

- For any i, j, k, m, p, q we have,

$$x_{ijkm}^{pq} = x_{jikm}^{pq} \qquad \bar{x}_{ijkm}^{pq} = -\bar{x}_{jikm}^{pq}$$

$$y_{ijkm}^{pq} = -y_{jikm}^{pq} \qquad \bar{y}_{ijkm}^{pq} = \bar{y}_{jikm}^{pq}$$

$$z_{ijkm}^{pq} = z_{jikm}^{pq} \qquad \bar{z}_{ijkm}^{pq} = -\bar{z}_{jikm}^{pq}$$

  and in particular, $\bar{x}_{iikm}^{pq} = y_{iikm}^{pq} = \bar{z}_{iikm}^{pq} = 0$
- Terms of the frequency series can be different from zero only when $i = j$ besides k and m are even.

Linsdtedt Poincaré Procedures. Halo

$$
\begin{aligned}
x(t) &= \alpha_1 e^{\lambda_0 t} + \alpha_2 e^{-\lambda_0 t} + \alpha_3 \cos(\omega_0 t + \phi) \\
y(t) &= \bar{k}_2 \alpha_1 e^{\lambda_0 t} - \bar{k}_2 \alpha_2 e^{-\lambda_0 t} + \bar{k}_1 \alpha_3 \sin(\omega_0 t + \phi) \\
z(t) &= \alpha_4 \cos(\omega_0 t + \phi)
\end{aligned}
$$

$$
\left\{
\begin{array}{rcl}
\ddot{x} - 2\,\dot{y} - (1 + 2c_2)\,x & = & \dfrac{\partial}{\partial x} \displaystyle\sum_{n \geq 3} c_n \rho^n P_n \left(\frac{x}{\rho} \right), \\
\ddot{y} + 2\,\dot{x} + (c_2 - 1)\,y & = & \dfrac{\partial}{\partial y} \displaystyle\sum_{n \geq 3} c_n \rho^n P_n \left(\frac{x}{\rho} \right), \\
\ddot{z} + c_2\,z & = & \dfrac{\partial}{\partial z} \displaystyle\sum_{n \geq 3} c_n \rho^n P_n \left(\frac{x}{\rho} \right) + \Delta\,z,
\end{array}
\right.
$$

Linsdtedt Poincaré Procedures. Halo

$$x(t) = \sum e^{(i-j)\theta_3} \left[x^p_{ijkm} \cos(p\theta_1) + \bar{x}^p_{ijkm} \sin(p\theta_1) \right] \alpha_1^i \alpha_2^j \alpha_3^k \alpha_4^m$$

$$y(t) = \sum e^{(i-j)\theta_3} \left[y^p_{ijkm} \cos(p\theta_1) + \bar{y}^p_{ijkm} \sin(p\theta_1) \right] \alpha_1^i \alpha_2^j \alpha_3^k \alpha_4^m$$

$$z(t) = \sum e^{(i-j)\theta_3} \left[z^p_{ijkm} \cos(p\theta_1) + \bar{z}^p_{ijkm} \sin(p\theta_1) \right] \alpha_1^i \alpha_2^j \alpha_3^k \alpha_4^m$$

where $\theta_1 = \omega t + \phi_1, \qquad \theta_3 = \lambda t$ and,
$\omega = \sum \omega_{ijkm} \alpha_1^i \alpha_2^j \alpha_3^k \alpha_4^m,$

$$\lambda = \sum \lambda_{ijkm} \alpha_1^i \alpha_2^j \alpha_3^k \alpha_4^m. \quad \Delta = \sum d_{ijkm} \alpha_1^i \alpha_2^j \alpha_3^k \alpha_4^m = \mathbf{0}.$$

Computational Time

order	15	17	19	21	23	25
Lissajous (secs)	1.71	4.91	12.9	32.2	75.3	167.7
halo (secs)	0.79	2.05	4.95	11.2	23.9	48.9

CPU time in seconds for Type I expansions under a Pentium IV 3.40GHz with 2GB RAM. Implemented in Fortran and using GNU compiler (g77 -O).

Tests on the Expansions

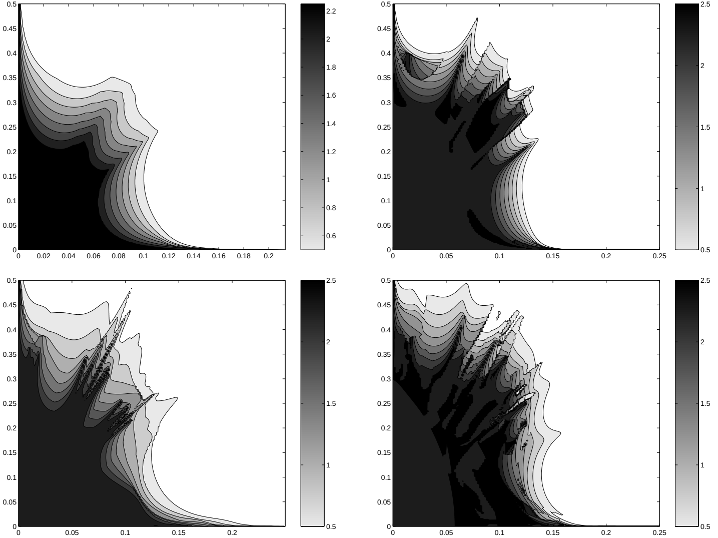

The 10^{-6} test. Columns order 9,15. Rows min and max agreement for all phases.

Tests on the Expansions

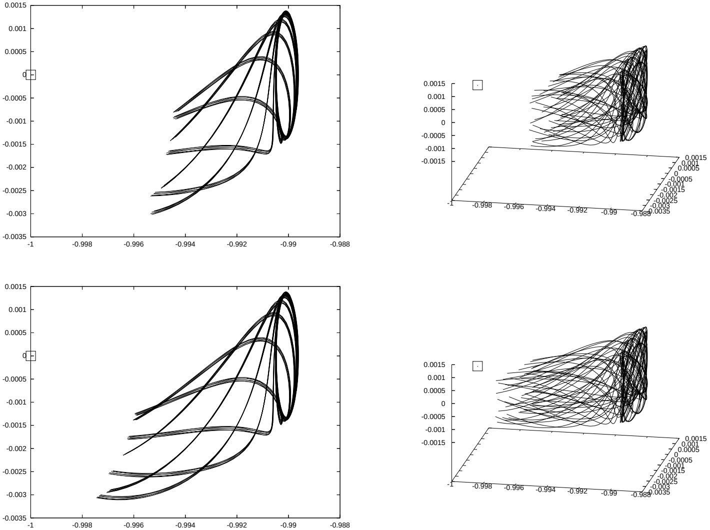

The 10^{-6} test for WS. Rows, order 9,15. $\alpha_3 = 0.042$, $\alpha_4 = 0.13$.

Tests on the Expansions

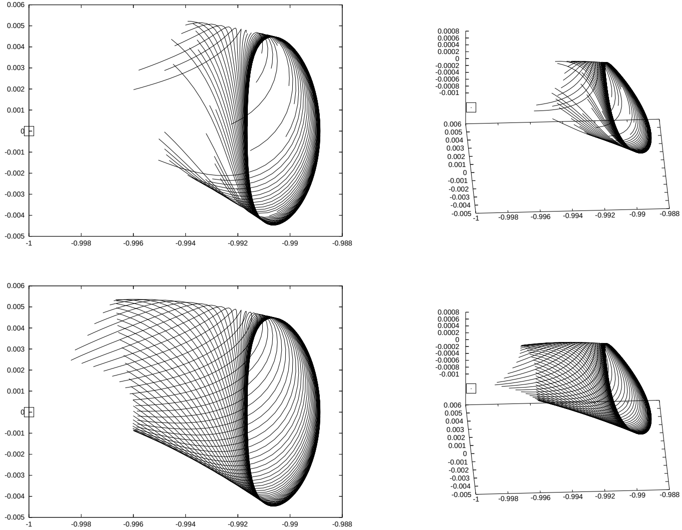

The 10^{-6} test for WU. Rows, order 9,15. $\alpha_4 = 0.08$.

Transfer Applications of Invariant Manifolds

- Impulsive direct transfers from Earth to LPO
  - Transfers to L_1 or L_2 in the Sun-Earth system
  - Transfers to L_1 or L_2 in the Earth-Moon system
- Low Thrust transfers to LPO
- Transfers inside L_1 the (or L_2) regime
  - Changing the size (amplitudes) of the orbit (impulsive, heteroclinic, low thrust)
  - Changing phases of stacks of satellites (impusive, homoclinic, heteroclinic, low thrust)
  - Eclipse Avoidance
- Transfers from L_1 to L_2 regime (or viceversa)
- Transfers from Earth-Moon to Sun-Earth LPO
- Other Low Energy Transfers (to the Moon, between Jovian Moons,...)
- Station Keeping

Transfer to Libration Point Orbits

Using orbits of the Stable Manifold and tending asimptotically to a Halo orbit.

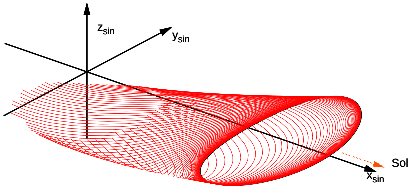

Manifolds provide cheap transfers to LPO.

Transfer to Libration Point Orbits

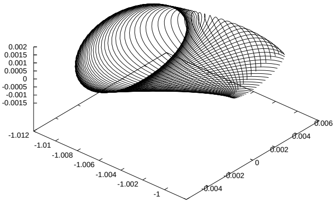

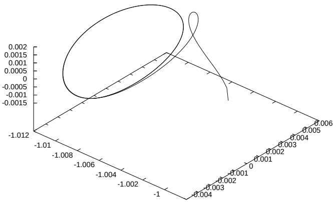

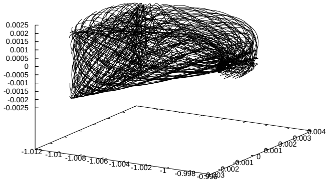

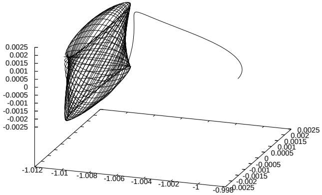

Low thrust transfer to L_1 Halo Sun-Earth

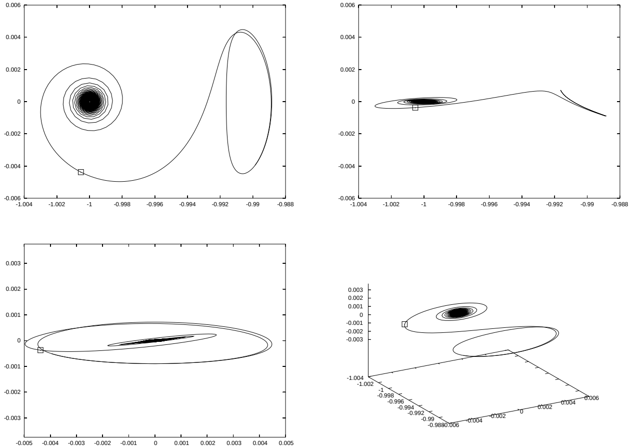

Looking for Simple LT transfers to SE Halo

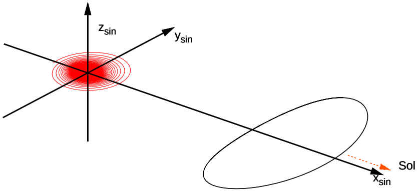

- Starting from LEO, we use a low-thurst engine.

Looking for Simple LT transfers to SE Halo

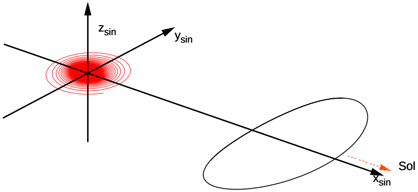

- And the trajectory spirals about the Earth.

Looking for Simple LT transfers to SE Halo

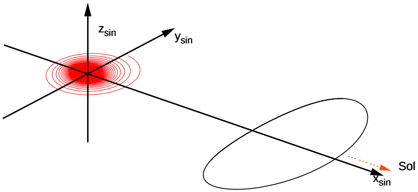

- And the trajectory spirals about the Earth.

Looking for Simple LT transfers to SE Halo

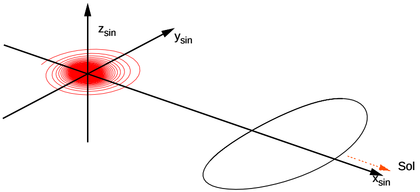

- And the trajectory spirals about the Earth.

Looking for Simple LT transfers to SE Halo

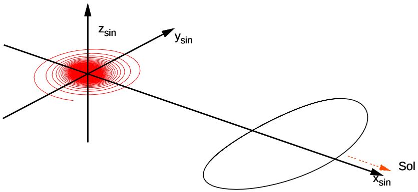

- And the trajectory spirals about the Earth.

Looking for Simple LT transfers to SE Halo

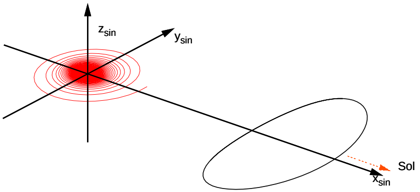

- And the trajectory spirals about the Earth.

Looking for Simple LT transfers to SE Halo

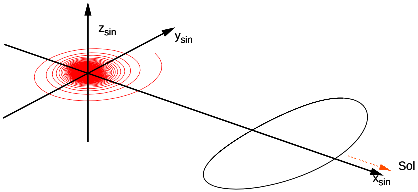

- And the trajectory spirals about the Earth.

Looking for Simple LT transfers to SE Halo

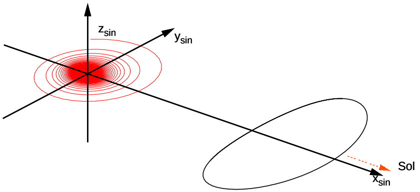

- And the trajectory spirals about the Earth.

Looking for Simple LT transfers to SE Halo

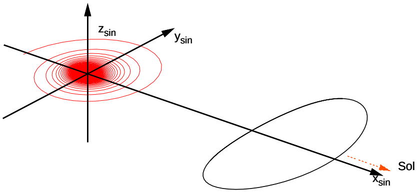

- And the trajectory spirals about the Earth.

Looking for Simple LT transfers to SE Halo

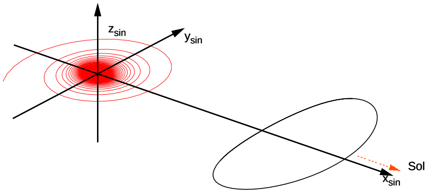

- And the trajectory spirals about the Earth.

Looking for Simple LT transfers to SE Halo

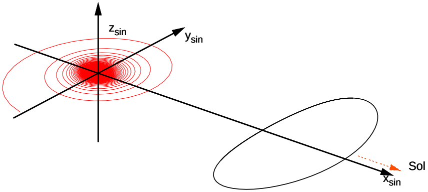

- And the trajectory spirals about the Earth.

Looking for Simple LT transfers to SE Halo

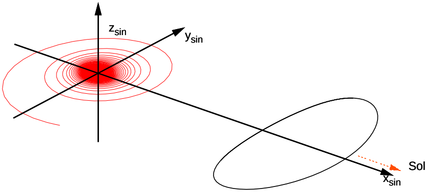

- And the trajectory spirals about the Earth.

Looking for Simple LT transfers to SE Halo

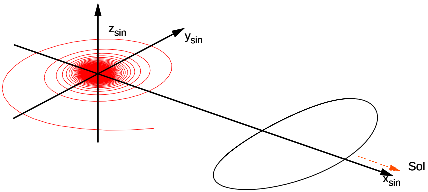

- And the trajectory spirals about the Earth.

Looking for Simple LT transfers to SE Halo

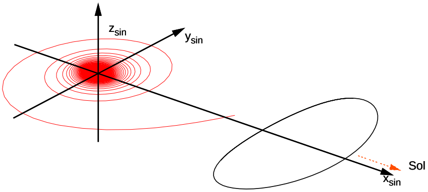

- We switch off thrust when we meet the stable manifold.

Looking for Simple LT transfers to SE Halo

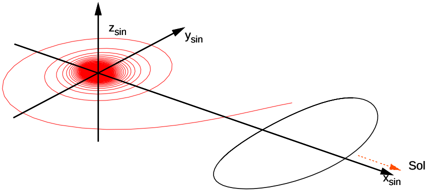

- The manifold provides the transfer to the Halo.

Looking for Simple LT transfers to SE Halo

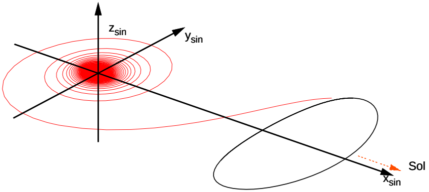

- The manifold provides the transfer to the Halo.

Looking for Simple LT transfers to SE Halo

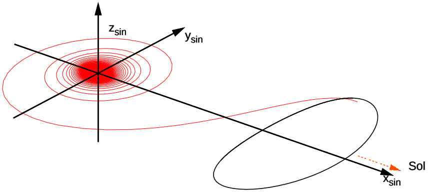

- The manifold provides the transfer to the Halo.

Looking for Simple LT transfers to SE Halo

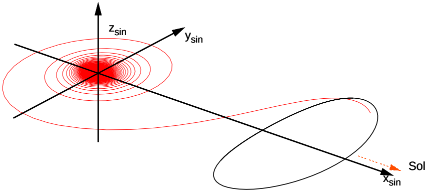

- The manifold provides the transfer to the Halo.

Looking for Simple LT transfers to SE Halo

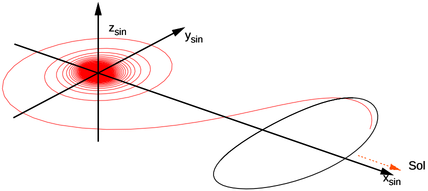

- The manifold provides the transfer to the Halo.

Looking for Simple LT transfers to SE Halo

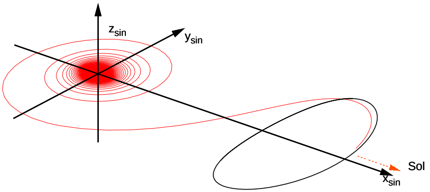

- The manifold provides the transfer to the Halo.

Looking for Simple LT transfers to SE Halo

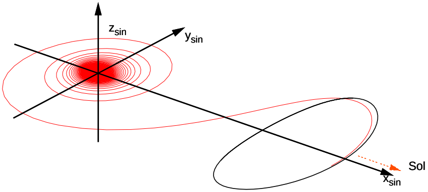

- The manifold provides the transfer to the Halo.

Looking for Simple LT transfers to SE Halo

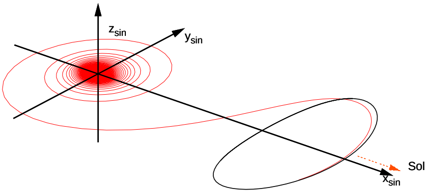

- The manifold provides the transfer to the Halo.

Computations using the DS Approach

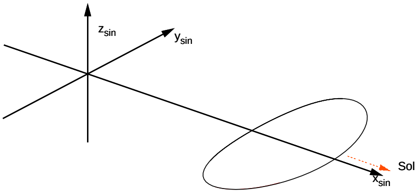

- We take initial conditions in the stable manifold

Computations using the DS Approach

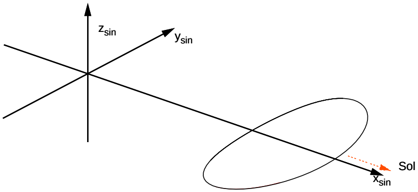

- We integrate backwards and propagate the manifold

Computations using the DS Approach

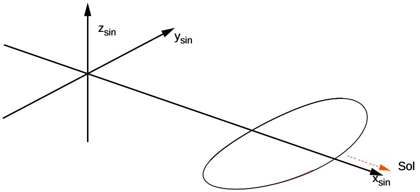

- We integrate backwards and propagate the manifold

Computations using the DS Approach

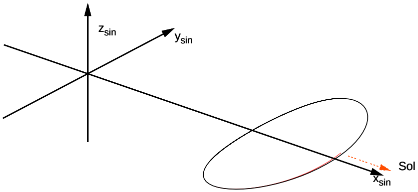

- We integrate backwards and propagate the manifold

Computations using the DS Approach

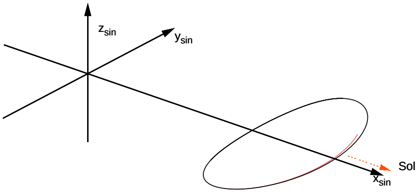

- We integrate backwards and propagate the manifold

Computations using the DS Approach

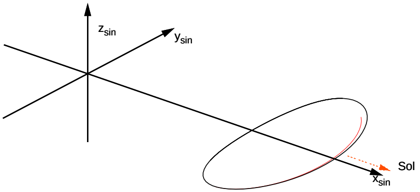

- We integrate backwards and propagate the manifold

Computations using the DS Approach

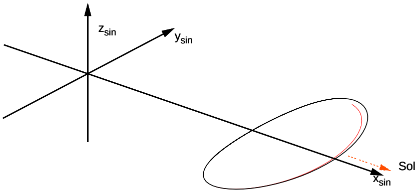

- We integrate backwards and propagate the manifold

Computations using the DS Approach

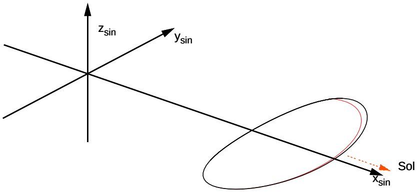

- We integrate backwards and propagate the manifold

Computations using the DS Approach

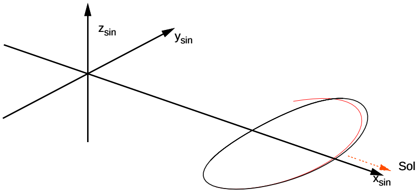

- We integrate backwards and propagate the manifold

Computations using the DS Approach

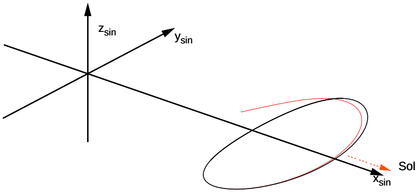

- We integrate backwards and propagate the manifold

Computations using the DS Approach

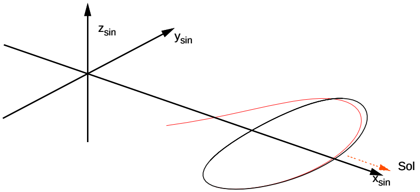

- We integrate backwards and propagate the manifold

Computations using the DS Approach

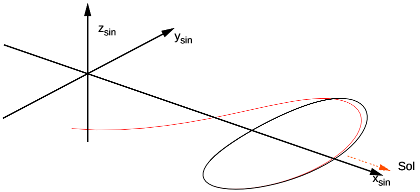

- We integrate backwards and propagate the manifold

Computations using the DS Approach

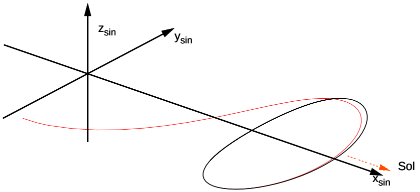

- After a given t_{coast} we integrate with thrust.

Computations using the DS Approach

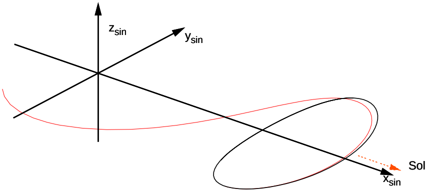

- Reaching a altitude 1000km above the Earth we stop the integration. And we compute the orbital elements of the departure orbit.

Computations using the DS Approach

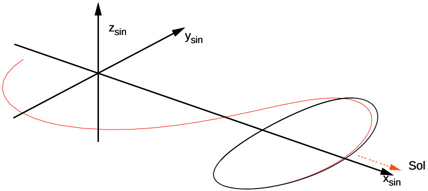

- Reaching a altitude 1000km above the Earth we stop the integration. And we compute the orbital elements of the departure orbit.

Computations using the DS Approach

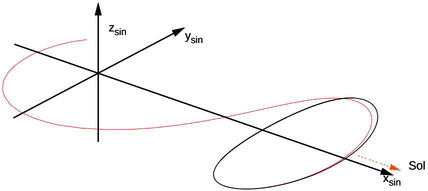

- Reaching a altitude 1000km above the Earth we stop the integration. And we compute the orbital elements of the departure orbit.

Computations using the DS Approach

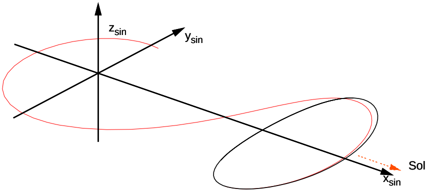

- Reaching a altitude 1000km above the Earth we stop the integration. And we compute the orbital elements of the departure orbit.

Computations using the DS Approach

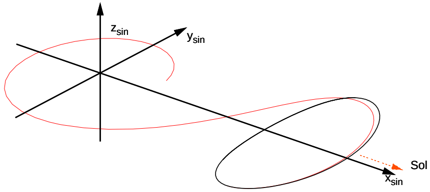

- Reaching a altitude 1000km above the Earth we stop the integration. And we compute the orbital elements of the departure orbit.

Computations using the DS Approach

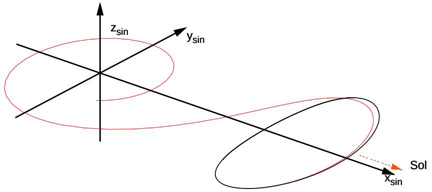

- Reaching a altitude 1000km above the Earth we stop the integration. And we compute the orbital elements of the departure orbit.

Computations using the DS Approach

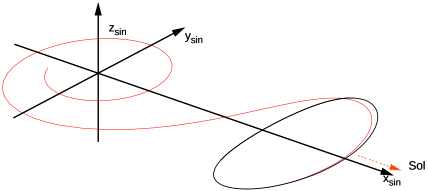

- Reaching a altitude 1000km above the Earth we stop the integration. And we compute the orbital elements of the departure orbit.

Computations using the DS Approach

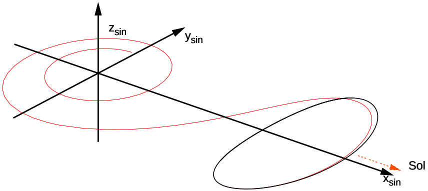

- Reaching a altitude 1000km above the Earth we stop the integration. And we compute the orbital elements of the departure orbit.

Computations using the DS Approach

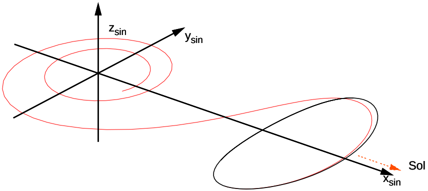

- Reaching a altitude 1000km above the Earth we stop the integration. And we compute the orbital elements of the departure orbit.

Computations using the DS Approach

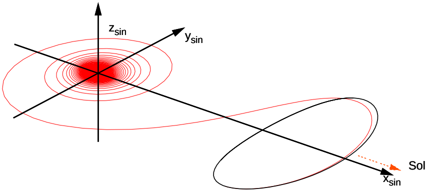

- Reaching a altitude 1000km above the Earth we stop the integration. And we compute the orbital elements of the departure orbit.

Computations using the DS Approach

Explorations:

- Let us consider the Sun–Earth+Moon (L_1 and L_2).
- We are interested in departure orbits with:
  - Low eccentricity.
  - Low inclination.
- Fixed Parameters:
  - Reference altitude: 1000km.
  - Intitial conditions on local stable manifold: $\alpha_2 = 10^{-3}$.
- Parameters to be changed and analized:
  - Phase in the Halo orbit $\rightarrow \phi$
  - Coasting time in the stable manifold $\rightarrow t_{coast}$
  - Thrust magnitude $\rightarrow F_T$
  - Halo orbit amplitude $\rightarrow \alpha_4$

Some Results and Regions with Low Eccentricity

Studies changing α_4 and F_T

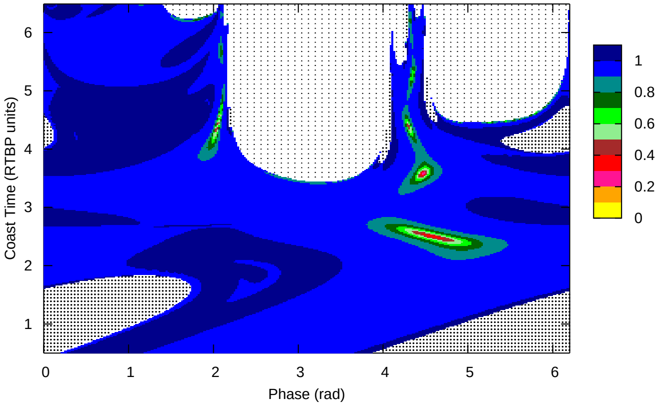

Some Results and Regions with Low Ecc.

Some examples of interesting transfers

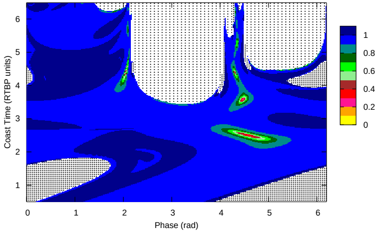

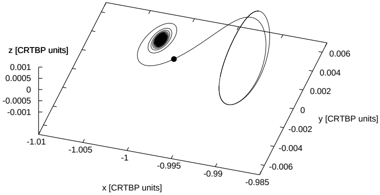

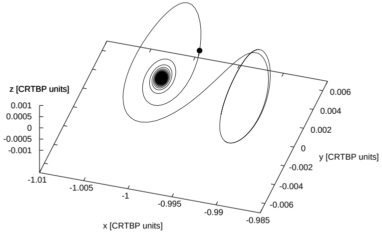

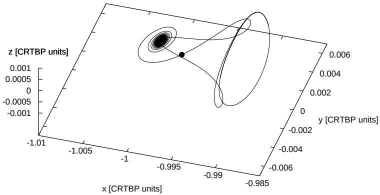

Some Results and Regions with Low Ecc.

Some examples of interesting transfers

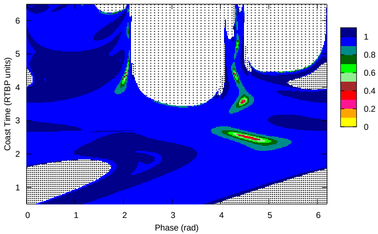

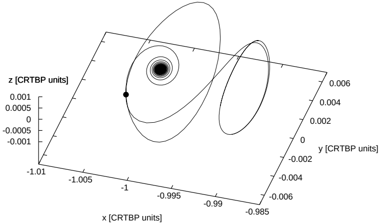

Some Results and Regions with Low Ecc.

Results for SEL2 are similar

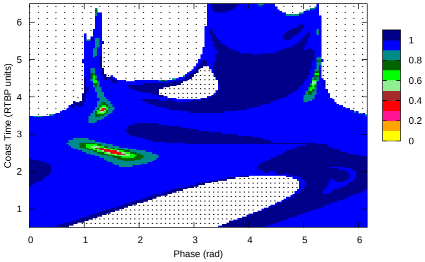

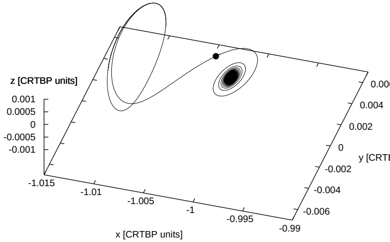

Influence of the parameters

Influence of the Halo Amplitude and of the Thrust Magnitude

- Inclination

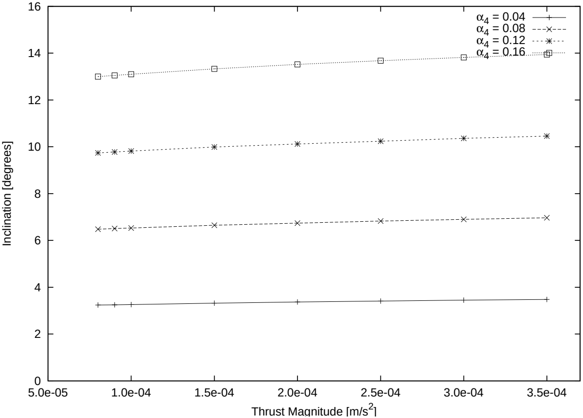

Influence of the parameters

Influence of the Halo Amplitude and of the Thrust Magnitude

- Total transfer time

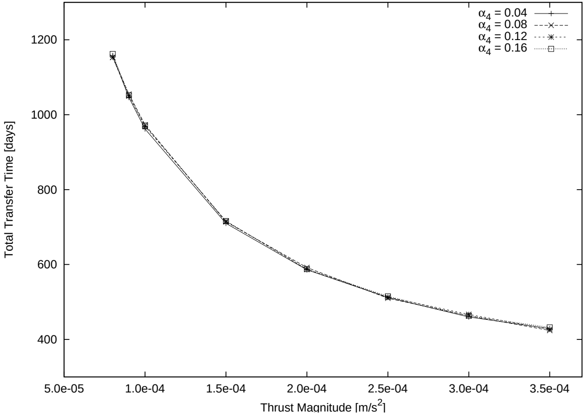

Influence of the parameters

Influence of the Halo Amplitude and of the Thrust Magnitude

- Time of thrust arc

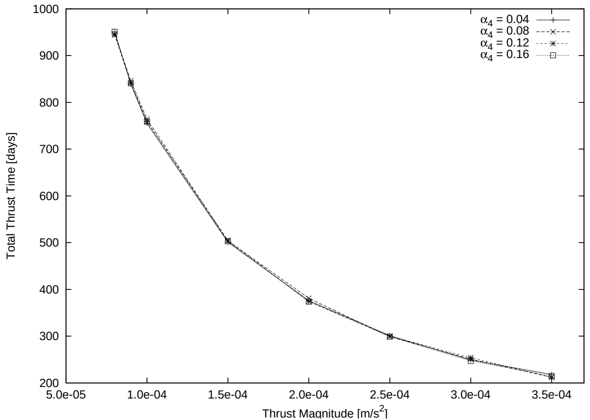

Studies in a Realistic Model

Main Perturbations taken into account:

- Gravitational Harmonics (coeffs. from EGM96 model)
- Atmospheric Drag (density model MSISE90)
- Solar Radiation Pressure (ct. Solar Rad coeff. 1AU)
- Other grav. perturbations (Moon, Planets ... JPL eph)

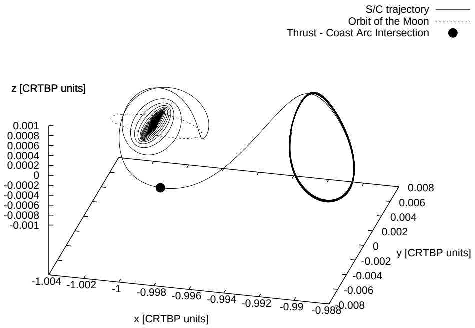

Low thrust transfer to Liss L_1 Sun-Earth

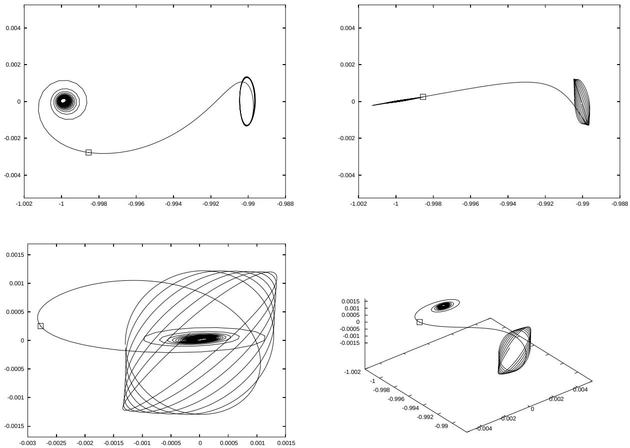

Transfers to Earth-Moon Lissajous LPO

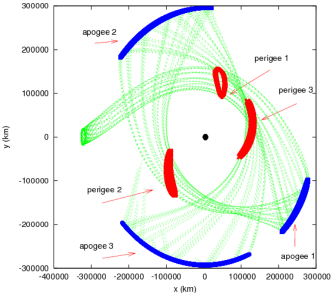

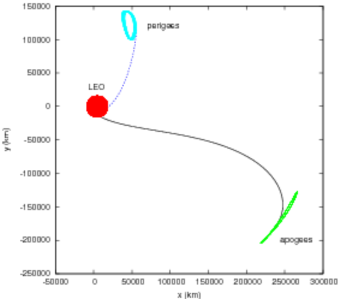

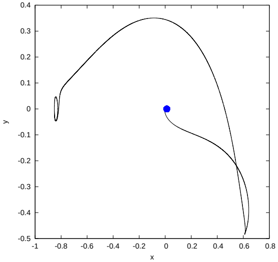

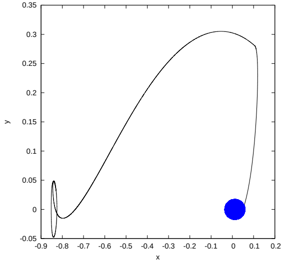

Low thrust transfer to Halo L_2 Earth-Moon

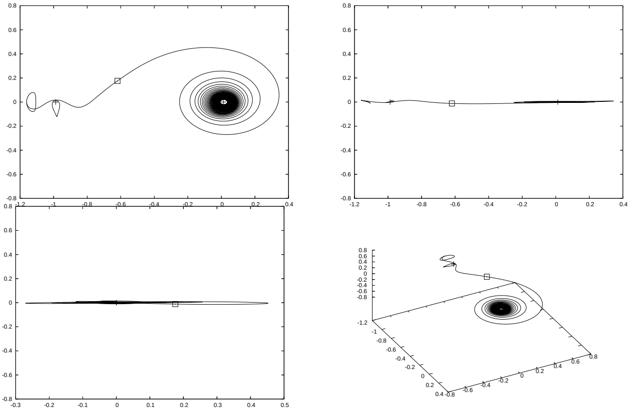

Eclipse Avoidance. LOEWE

(A particular transfer between Lissajous orbits)

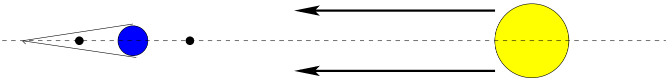

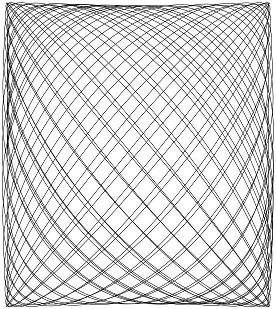

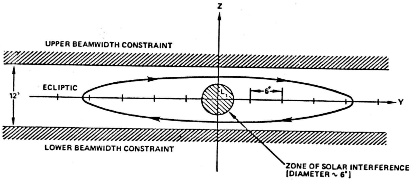

Eclipse Avoidance. LOEWE

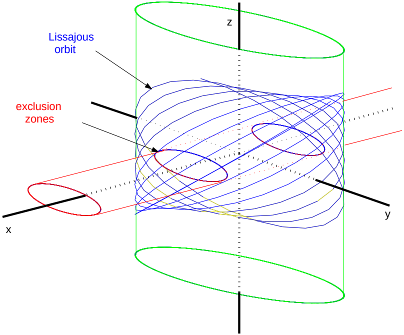

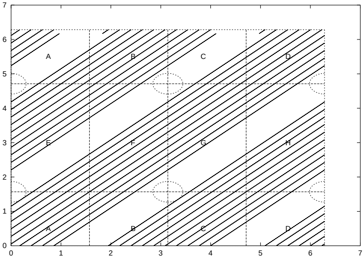

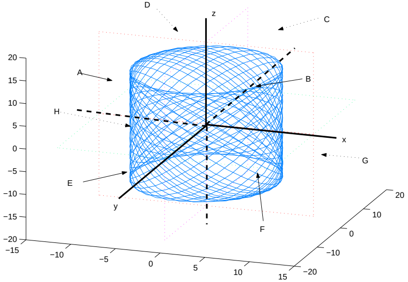

Eclipse Avoidance. LOEWE

Effective Phases

Considering the angular variables of the torus,

$$\Phi = \omega t + \phi, \quad \Psi = \nu t + \psi, \quad (\mathrm{mod}\ 2\pi).$$

The exclusion zone appears as,

$$y^2 + z^2 < R^2,$$

Using linear equations:

$$\bar{k}^2 A_x^2 \sin^2 \Phi + A_z^2 \cos^2 \Psi = R^2$$

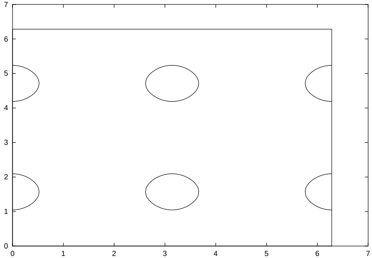

Eclipse Avoidance. LOEWE

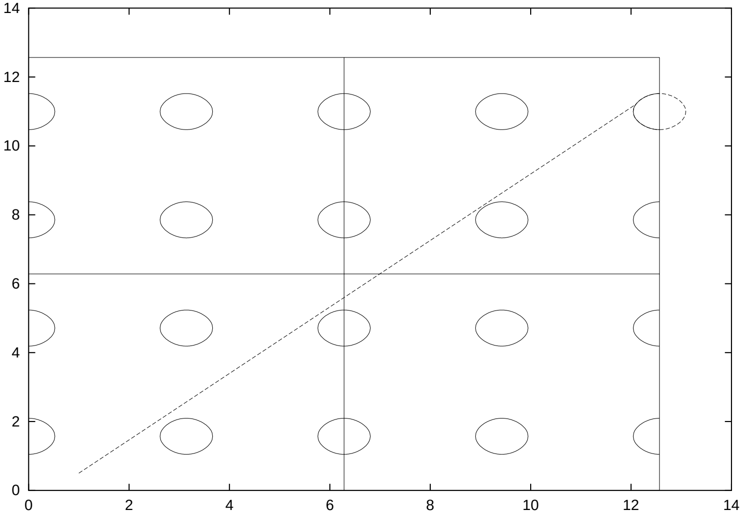

Eclipse Avoidance. LOEWE

	ω	ν	ν/ω	usual R (km)	angle from Earth
L_1	2.086	2.015	0.966	90000	$\simeq$ 3.5 deg radius
L_2	2.057	1.985	0.965	14000	$\simeq$ 0.54 deg radius

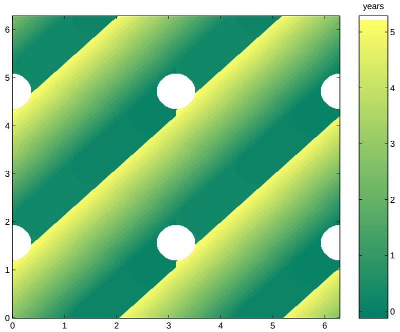

L_1 case $A_y = A_z = 250000$ km, $R = 90000$ km.

Eclipse Avoidance. LOEWE

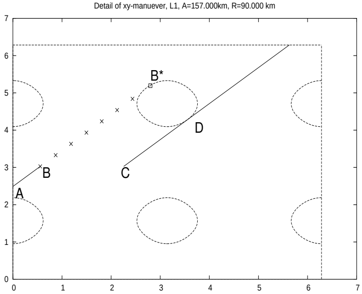

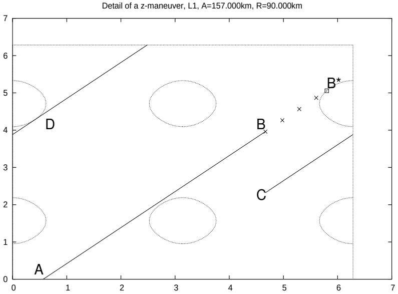

Essentially, manoeuvres are seen as jumps of the straight trajectory in the EPP. They look as horizontal or vertical displacements, depending on whether in-plane or out-of-plane manoeuvres are applied. These type of manoeuvres have symmetrical properties too and this makes their planning very easy.

Eclipse Avoidance. LOEWE

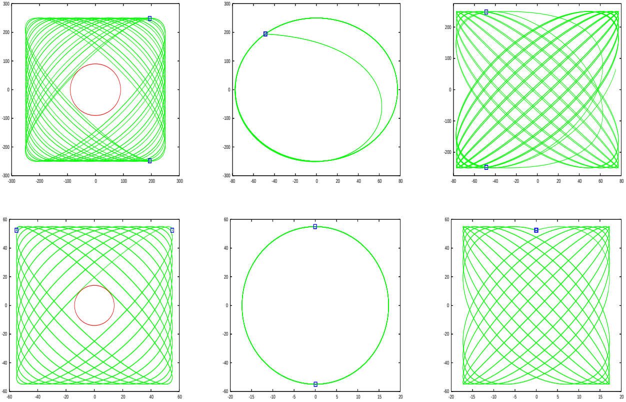

First row, example of one-sided cycle. Trajectory around L_1 with $A = 250000$ km, $R = 90000$ km (xy-maneuvers). Second row, example of two-sided cycle. Trajectory about L_2 with with $A = 55000$ km, R=14000 km. (z-maneuvers).

Homoclinic and Heteroclinic orbits

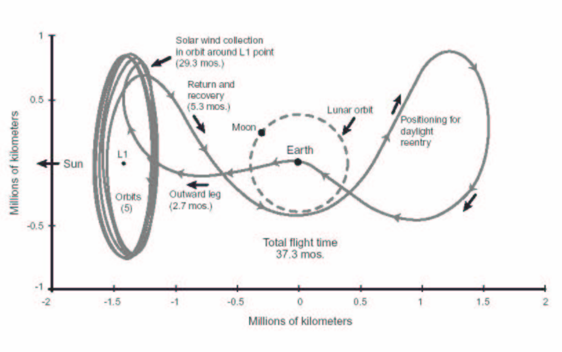

Mission Trajectory

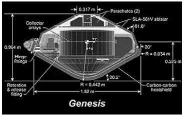

Homoclinic and Heteroclinic orbits

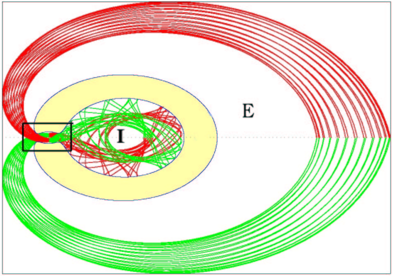

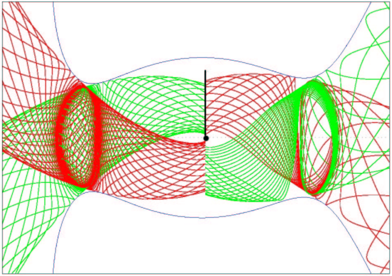

Homoclinic and Heteroclinic orbits

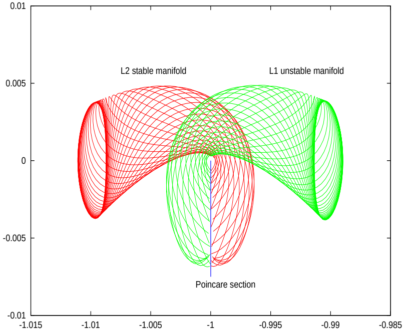

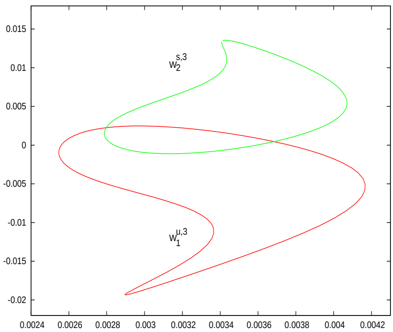

Sun-Earth problem. (left) Hyperbolic manifolds associated with the Lyapunov orbits around L_1 and L_2, $\mathcal{C}$=3.00085. (right) Poincaré section cuts of L_1 and L_2 manifolds (both at the third cut) $\mathcal{C}$=3.00089.

Homoclinic and Heteroclinic orbits

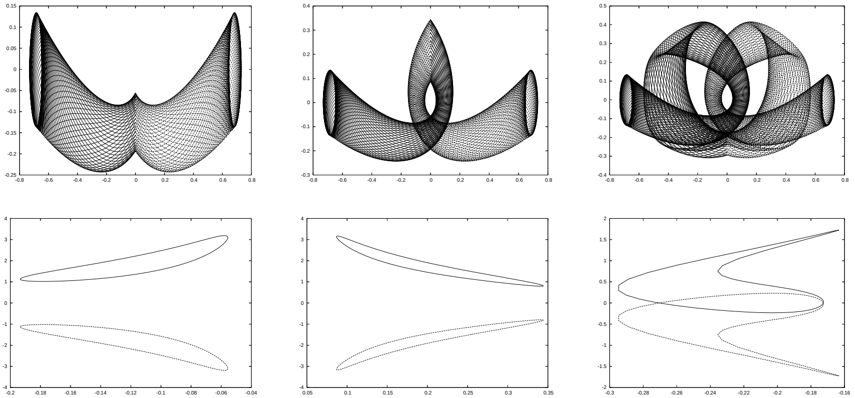

Homoclinic and Heteroclinic orbits

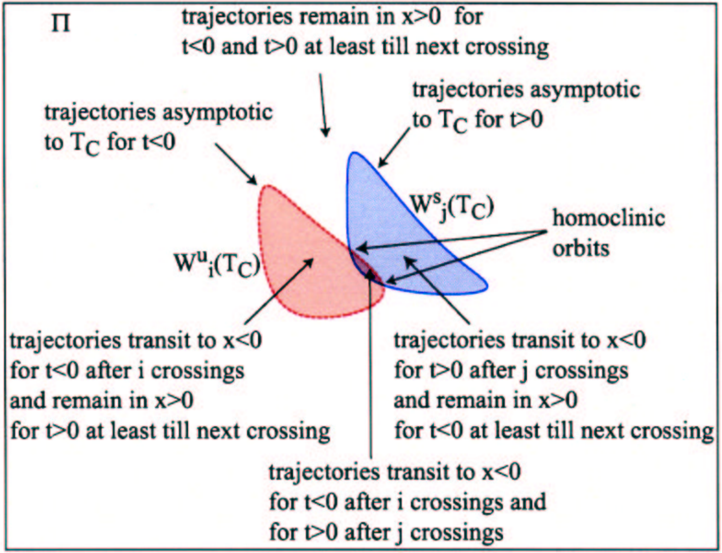

Homoclinic and Heteroclinic orbits

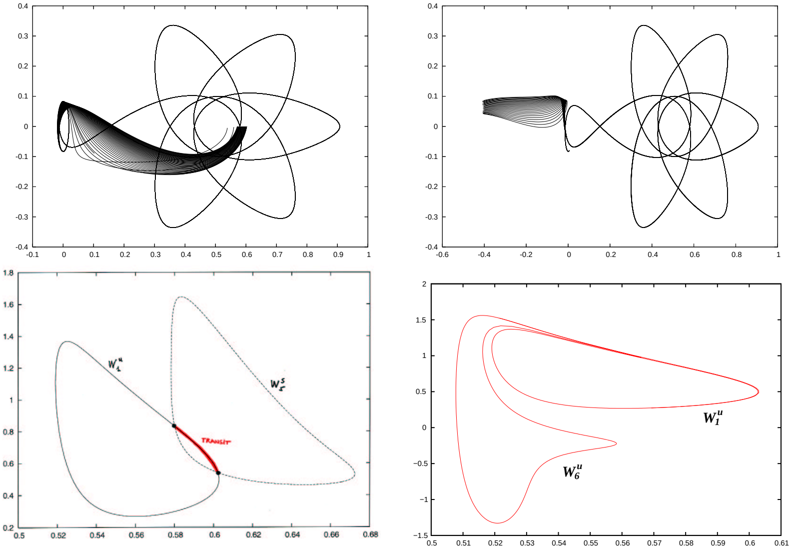

Homoclinic and Heteroclinic orbits

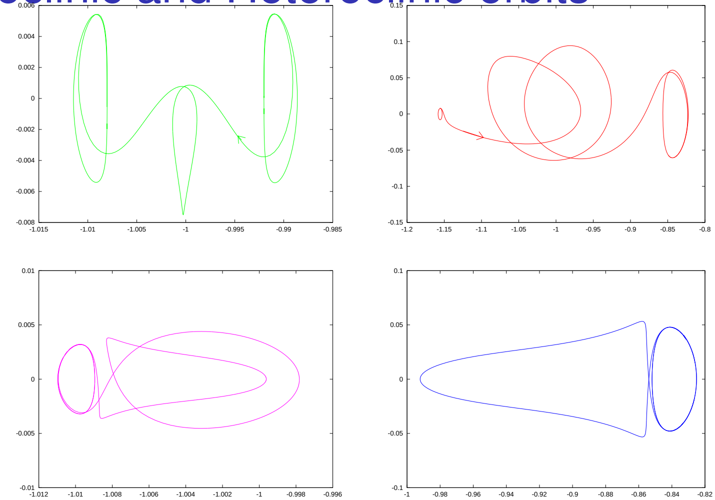

Some examples of homoclinic and heteroclinic connections of the planar RTBP. (Left, Sun-Earth. Right, Earth-Mooon).

Homoclinic and Heteroclinic orbits

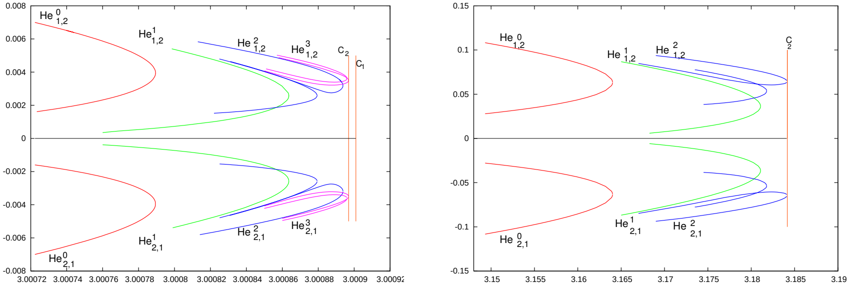

Families of heteroclinic connections. Left Sun-Earth and right Earth-Moon cases.

Homoclinic and Heteroclinic orbits

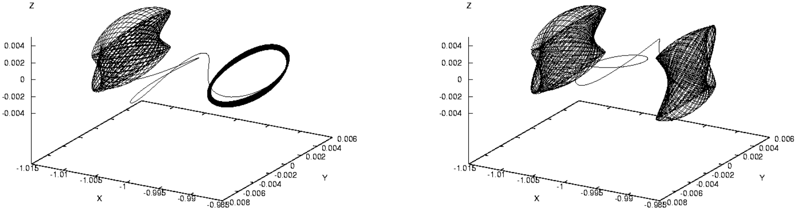

L_1-L_2 heteroclinic connections: (left) between a Lissajous orbit around L_2 and a quasi-halo orbit around L_1. (right) between two Lissajous orbits.

Computation of 3D Heteroclinic orbits

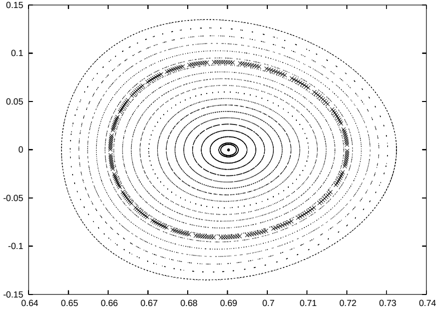

Let us consider the computation of heteroclinic orbits from the L_2 region to the torus of Lindstedt amplitudes $\alpha_3 = 0.042$, $\alpha_4 = 0.13$ (200×10^3 km both in Y and Z amplitudes) about L_1 in the Hill's problem.

Computation of 3D Heteroclinic orbits

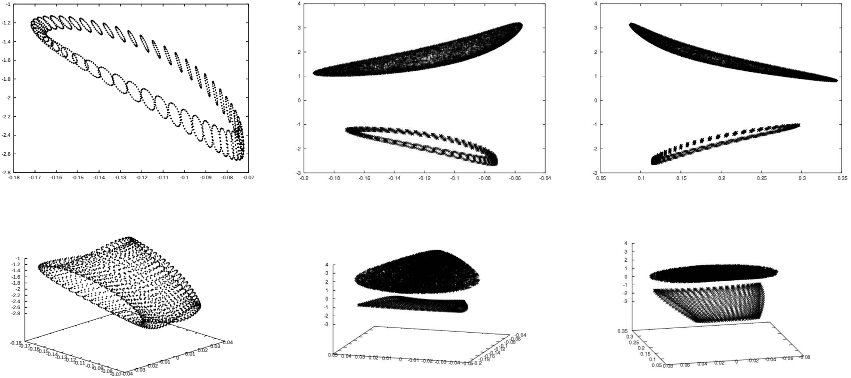

$Y\dot{Y}$ and $YZ\dot{Y}$ Poincaré sections at $X = 0$ of the corresponding manifolds. (No turn (central) and one turn (right) about the primary).

Computation of 3D Heteroclinic orbits

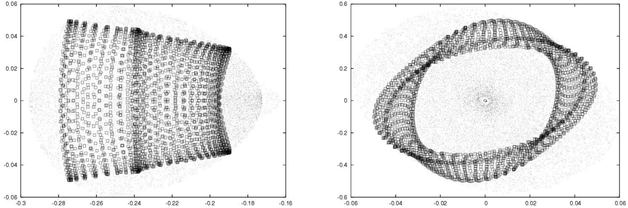

Third encounters, YZ and $Z\dot{Z}$ projections.

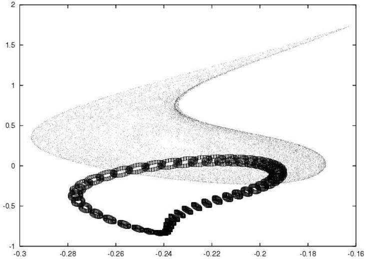

Third encounters, $Y\dot{Y}$ projection.

Computation of 3D Heteroclinic orbits

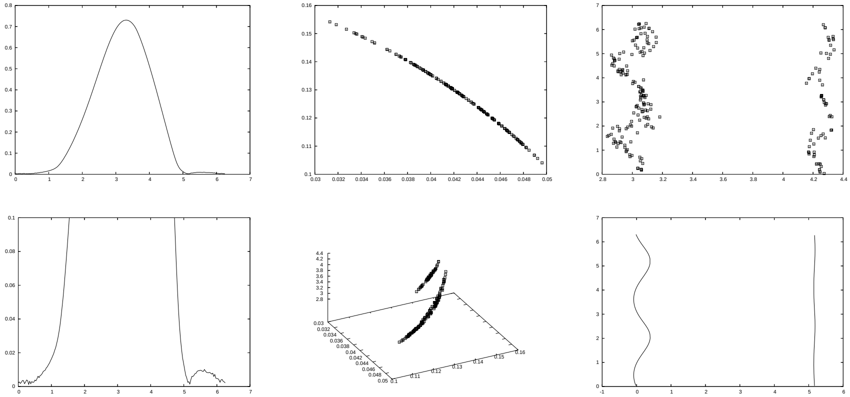

Computation of 3D Heteroclinic orbits

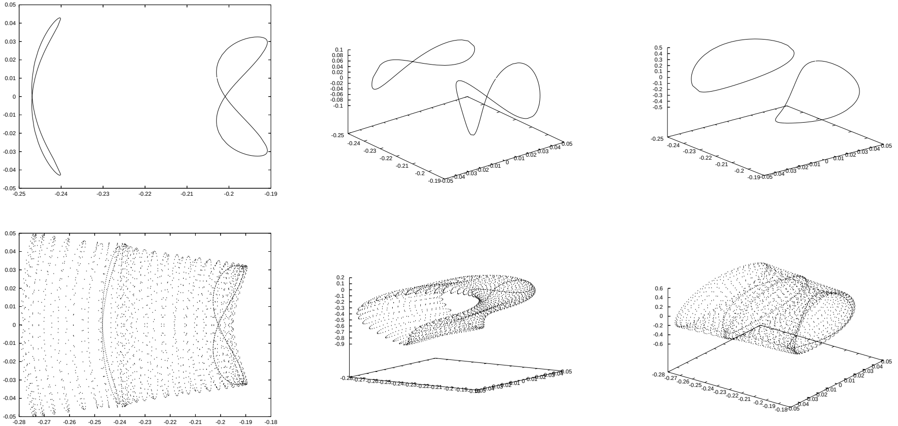

YZ, $YZ\dot{Y}$ and $YZ\dot{Z}$ projections of the heteroclinic points at the Poincaré section $X = 0$.

Computation of 3D Heteroclinic orbits

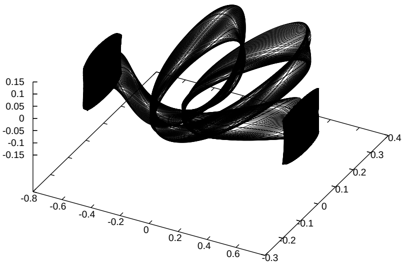

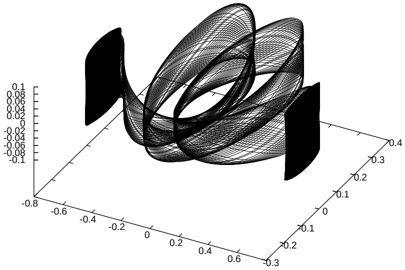

Heteroclinic families obtained

Other examples of Heteroclinic orbits

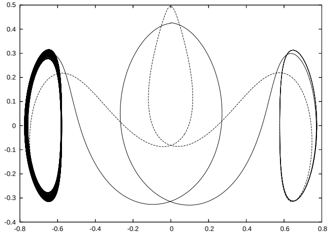

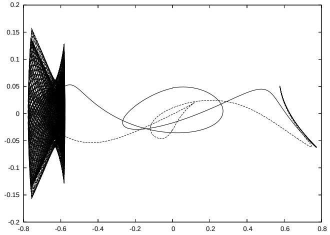

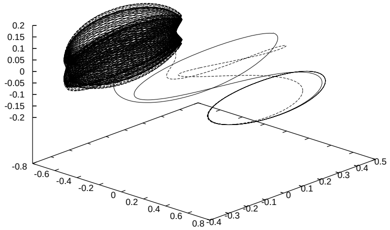

Heteroclinic 3D inside the Energy level

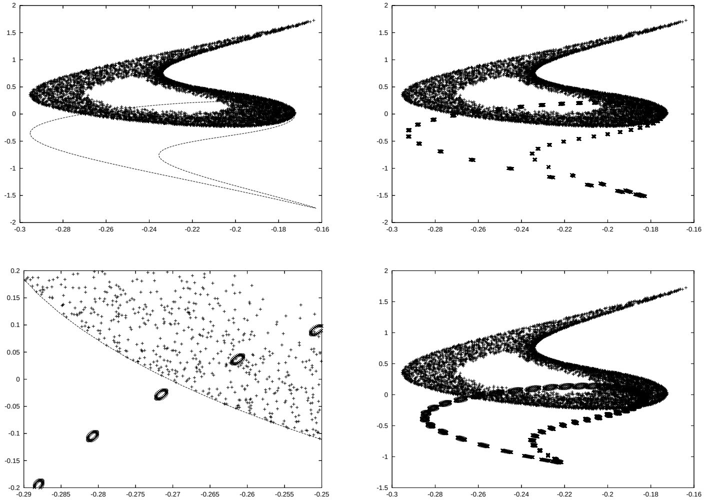

$(Y, \dot{Y})$ Poincaré section for out-of-plane amplitudes 0.00, 0.050 and 0.1 in the energy level CJ=4.26460693

Heteroclinic 3D inside the Energy level

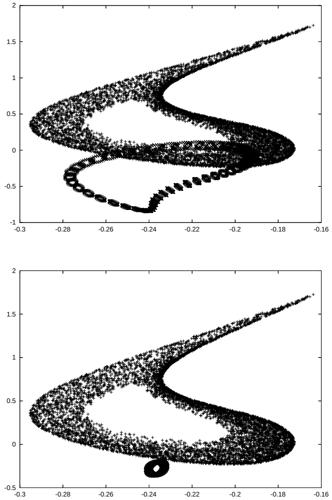

$(Y, \dot{Y})$ Poincaré section for out-of-plane amplitudes 0.13, 0.16 and 0.1799 in energy level CJ=4.26460693

Heteroclinic 3D inside the Energy level

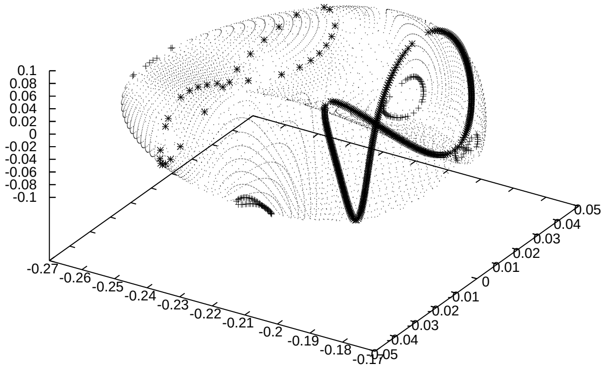

$(Y, Z, \dot{Y})$ projection at in the Poincaré section of the S^2 sphere of heteroclinic orbits for CJ=4.26460693

Heteroclinic 3D inside the Energy level

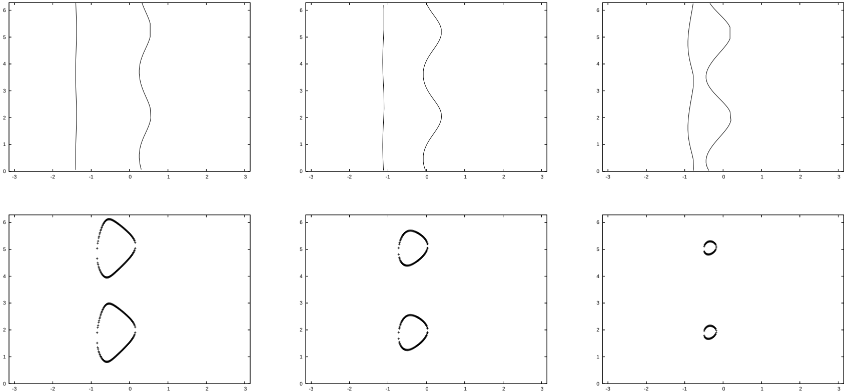

Evolution of the LP in-plane and out-of-plane phases in the S^2 sphere of connections giving transit and non transit orbits.

The Earth-Moon Gateway Station

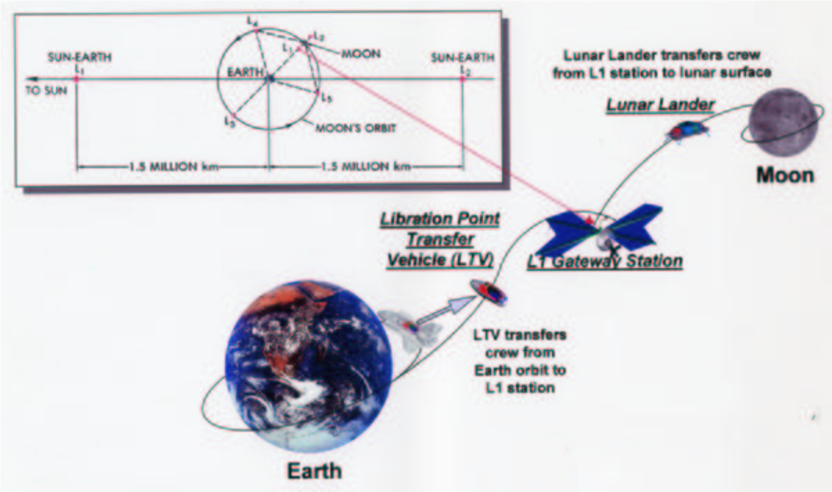

New Issues...

- The Sun-Earth and the Earth-Moon orbits are not coplanar
- The problem is not autonomous
- Scaling is different in Sun-Earth and in Earth-Moon
- The Earth-Moon part is strongly perturbed
- There are resonances between frequencies
- Need to compute real solutions for complete ephemeris

Sun-Earth and Earth-Moon reference frames

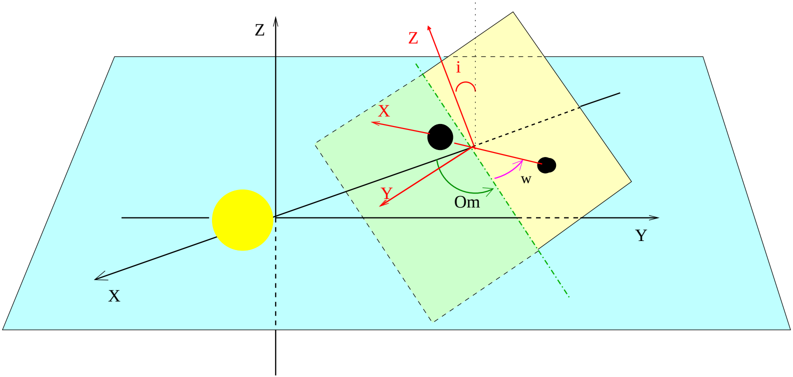

Poincaré Section $X = -1 + \mu$, Sun-Earth

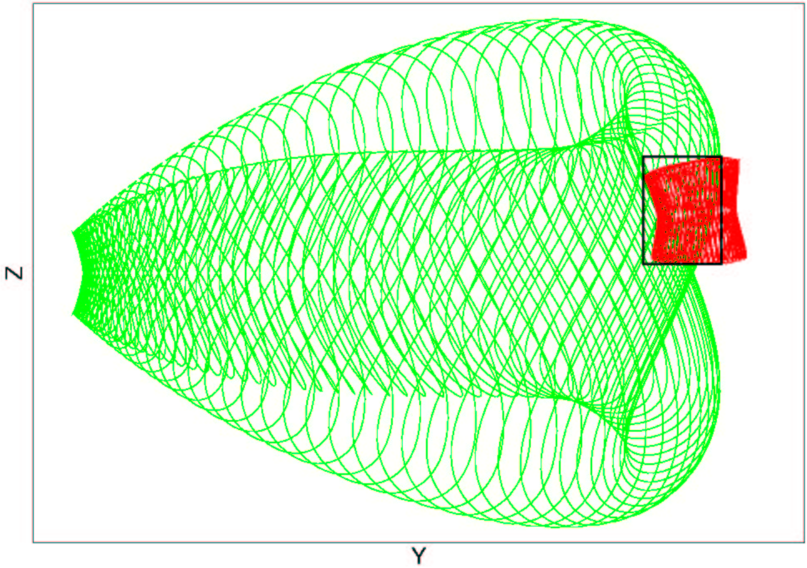

Poincaré Section $X = -1 + \mu$, Sun-Earth

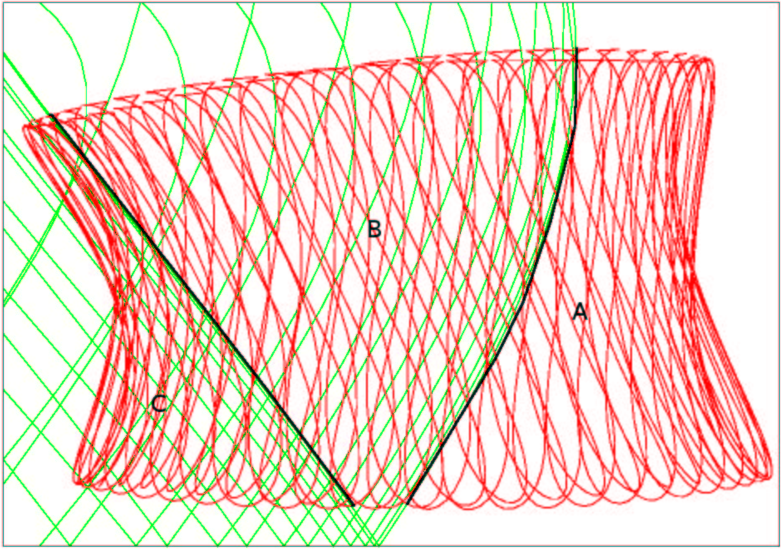

Sections and Earth-Moon angular variables

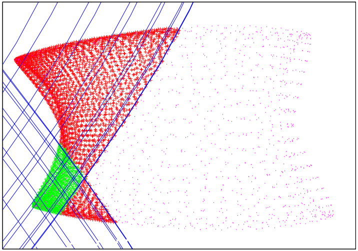

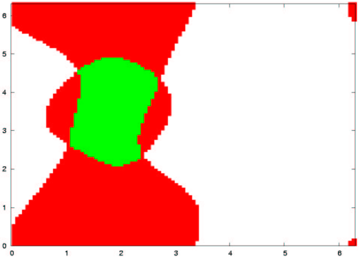

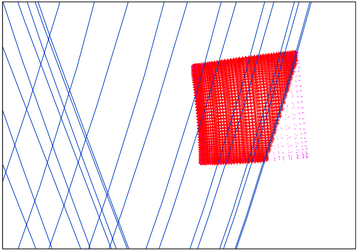

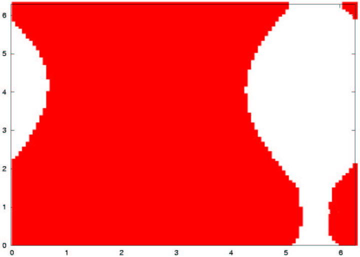

Sections and Earth-Moon angular variables

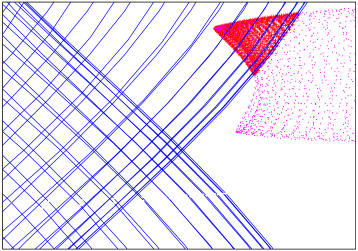

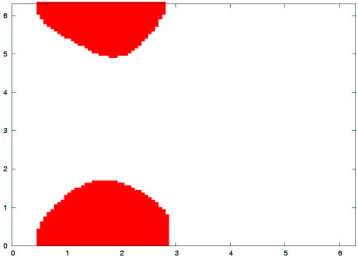

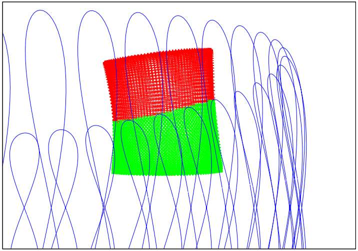

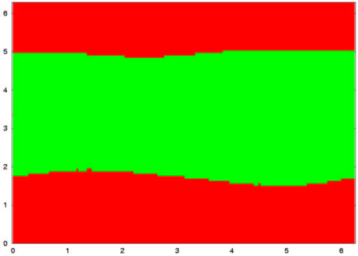

Sections and Earth-Moon angular variables

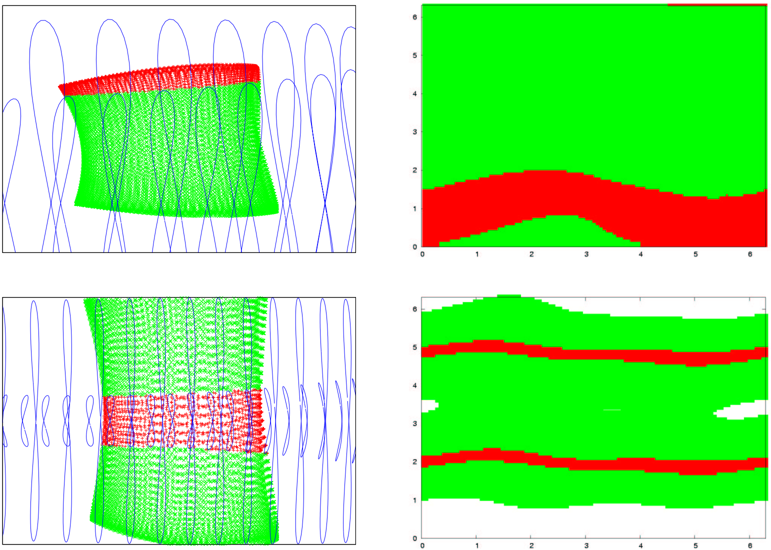

Ex. of connection with 4 possible maneuvres

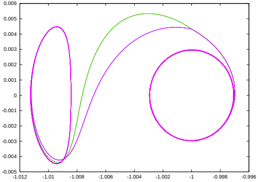

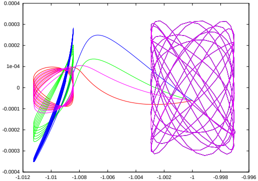

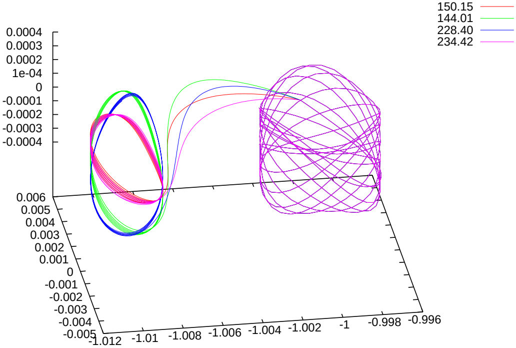

Ex. of connection with 2 possible maneuvres

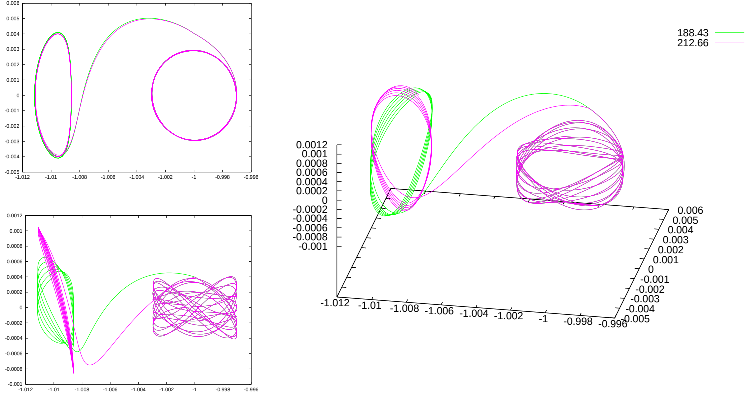

Refinement to JPL coordinates

1. The problem is no longer autonomous. The epoch at which the problems are coupled has to be chosen.

2. Apply multiple shooting to the SE and EM legs separately.

3. The position coordinates in the coupling point change $\rightarrow$ fix the initial point in the SE leg to be equal to the final point of the EM side.

4. Trajectories in JPL coordinates with a Δv in the coupling point are obtained. (Δv is of the same order as in the uncoupled RTBPs).

From RTBP to JPL with a Δv

Red: RTBP, Green: JPL

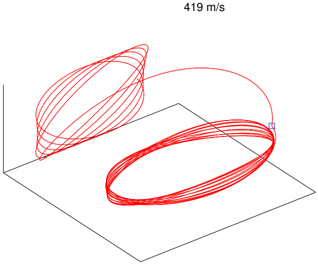

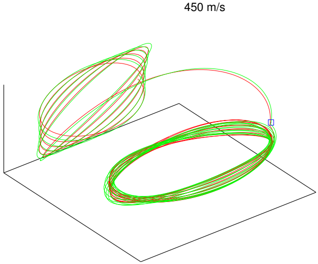

$A_x^{SE} = 10^5,\ A_z^{SE} = 3.2\ 10^5,\ A_x^{EM} = 6500,\ A_z^{EM} = 2\ 10^4 (km),\ \alpha = 50^\circ,\ \beta = 40^\circ$

From RTBP to JPL with a Δv

Red: RTBP, Green: JPL

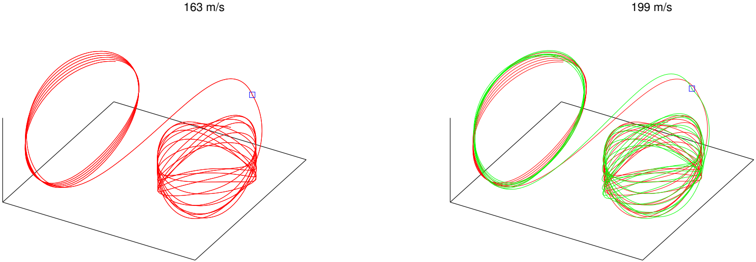

$$A_x^{SE} = 2.44\ 10^5,\ A_z^{SE} = 7.5\ 10^4,\ A_x^{EM} = 5250,\ A_z^{EM} = 1.6\ 10^4 (km),\ \alpha = 15^\circ,\ \beta = 105^\circ$$

Refinement to zero cost transfer trajectories

- Goal: reduce the Δv in the coupling point.
- New multiple shooting equations:

$$F\begin{pmatrix} Q_0^j \\ Q_1^j \\ \vdots \\ Q_{N-1}^j \\ Q_N^j \\ \vdots \\ Q_{N+M-1}^j \end{pmatrix} = \begin{pmatrix} \Phi(Q_0^j) \\ \Phi(Q_1^j) \\ \vdots \\ \Phi(Q_{N-1}^j) \\ \Phi(Q_N^j) \\ \vdots \\ \Phi(Q_{N+M-1}^j) \end{pmatrix} - \begin{pmatrix} Q_1^j \\ Q_2^j \\ \vdots \\ Q_N^j \\ Q_{N+1}^j \\ \vdots \\ Q_{N+M}^j \end{pmatrix} - \begin{pmatrix} 0 \\ 0 \\ \vdots \\ \Delta^j \\ 0 \\ \vdots \\ 0 \end{pmatrix} = \begin{pmatrix} 0 \\ 0 \\ \vdots \\ 0 \\ 0 \\ \vdots \\ 0 \end{pmatrix}$$

with $\Delta^j = (0, 0, 0, \Delta v_j)^T \in \mathbb{R}^6$ and $\|\Delta v_j\| < \|\Delta v_{j-1}\| \quad \forall j \geq 1$

Results of the refinement to zero cost

1. Zero cost connecting trajectories which keep the characteristics of the original trajectory in the RTBPs.

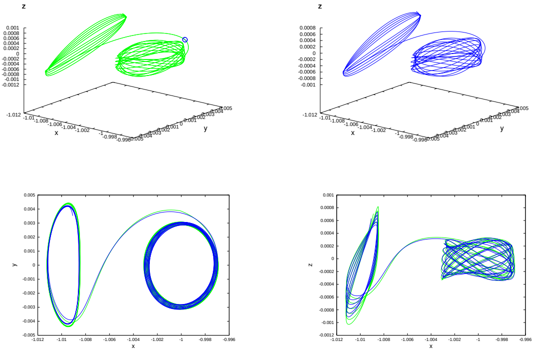

$A_x^{SE} = 2.13\ 10^5,\ A_z^{SE} = 7.5\ 10^4,\ A_x^{EM} = 2950,\ A_z^{EM} = 9000\ (km),\ \alpha = 60^\circ,\ \beta = 45^\circ$

Results of the refinement to zero cost

2 Zero cost connecting trajectories which are significantly different from the original seed in RTBP coordinates.

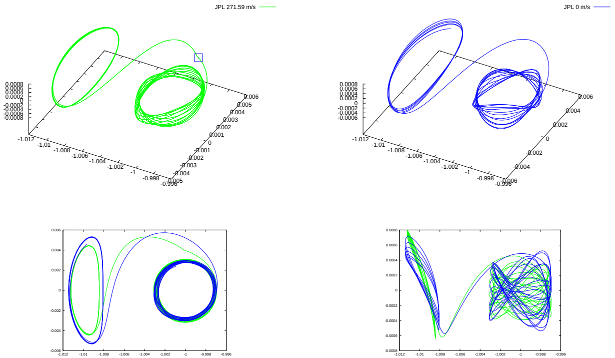

$A_x^{SE} = 2.13\ 10^5,\ A_z^{SE} = 7.5\ 10^4,\ A_x^{EM} = 5250,\ A_z^{EM} = 1.6\ 10^4 (km),\ \alpha = 10^\circ,\ \beta = 100^\circ$

Results of the refinement to zero cost

3. No zero cost transfer obtained. The manoeuvre is always reduced to less than 100 m/s.

Results of the refinement to zero cost

3 No zero cost transfer obtained. The manoeuvre is always reduced to less than 100 m/s.

Remark:

- Best behaviour in the refinement: SE Lissajous with big A_x amplitudes ($2\ 10^5$ km) and small A_z amplitudes (less than 10^5 km).

References

- Dynamics and mission design near libration point orbits, vol. 1-3. G. Gómez, R. Martínez, J. Llibre, C. Simó. World Sci. 2001.
- Dynamics and mission design near libration point orbits, vol. 1-3. G. Gómez, A. Jorba, J.J. Masdemont, C. Simó. World Sci. 2001.
- Connecting orbits and invariant manifolds in the spatial restricted three body problem. G. Gómez W.S. Koon, M.W. Lo, J. E. Marsden, J.J. Masdemont, S.D. Ross. Nonlinearity, 17:1571-1606, 2004.
- High order expansions of invariant manifolds of libration point orbits with applications to mission design. J.J. Masdemont. Dynamical Systems: an International Journal, 20(1):59-113, (2005).

References

- Assesment of Mission Design Including Utilization of Libration Points and Weak Stability Boundaries. E. Canalias, G. Gómez, M. Marcote, J.J Masdemont. Ariadna Final Report. `http://www.esa.int/gsp/ACT`, 2004.
- Impulsive Transfers between Lissajous Libration Point Orbits. E. Canalias, J. Cobos, J.J. Masdemont. Journal of the Astronautical Sciences, 51, 361-390, 2004.
- Homoclinic and Heteroclinic Transfer Trajectories between Planar Lyapunov Orbits in the Sun-Earth and Earth-Moon Systems. E. Canalias, J.J. Masdemont. Discrete and Continuous Dynamical Systems, 14, 261-279, 2006.
- Low Thrust Transfers from the Earth to Halo Orbits around the Libration Points of the Sun-Earth/Mooon System. P. Donato, J.J. Masdemont, P. Paglione, A.F. Prado. Proceedings of COBEM 2007.

References

- Geometry of Homoclinic Connections in a Planar Circular Restricted Three-Body Problem.
  M. Gidea, J.J. Masdemont. International Journal of Bifurcation and Chaos, 17, 1151-1159, 2007.
- Computation of Heteroclinic Orbits between Normally Hyperbolic Invariant 3-Spheres foliated by 2-Dimensional Invariant Tori in Hill's Problem. L. Arona, J.J. Masdemont. Discrete and Continuous Dynamical Systems. Supl. 2007.
- Computing natural transfers between Sun-Earth and Earth-Moon Lissajous libration point orbits. E. Canalias, J.J. Masdemont. Acta Astronautica. 63, 238-248, 2008.
- Leaving and reaching the Moon from a Libration Point Orbit E.M. Alessi, G. Gómez, J.J. Masdemont. To appear in Communications in Nonlinear Science and Numerical Simulation.